"Progress in Science and Engineering of Composites"
T. Hayashi, K. Kawata & S. Umekawa, Ed., ICCM-IV, Tokyo, 1982.

Damage and Fracture of Tridirectional Composites

P. Ladeveze, M. Poss, L. Proslier

Laboratoire de Mécanique et Technologie, E.N.S.E.T., 61, Avenue du Président Wilson, 94230 Cachan, France

ABSTRACT

This paper concerns damage and fracture of tridirectional composite materials. Damage phenomenon is defined as progressive deterioration of loaded materials, due to initiation and development of micro-voids and micro-cracks (2). Here it acts on the elastic modulus of the material.

It is impossible to obtain a simple sollicitation of traction or compression. The presence of defects due to the making of the specimens induces important bending effects. Consequently they are taken into account in the experimental method. The tested material is a tridirectional Carbon-Carbon composite.

From these tests a mathematical model is built up and verified. It is elastoplastic with isotropic hardening and anisotropic damage.

INTRODUCTION

Tridirectional composite materials with periodic structure have a complex mechanical behaviour due to their inhomogeneity and their anisotropic and tridimensional type. However the simplicity of geometry make easier the approach of phenomenons which are at theorigin of this behaviour.

Their industrial applications require a good comprehension of rupture and damage. For this, it is necessary to have a coherent experimental analysis and a simple modelisation of behaviour.

This work, supported by S.N.I.A.S. AEROSPATIALE, concerns the non-linear behaviour of tridirectional composites applied to Carbon-Carbon materials. We present successively the description of material, the experimental method, the formulation of model and its verification.

DESCRIPTION OF MATERIAL

It is a Carbon-Carbon composite of the S.N.I.A.S. AEROSPATIALE. It is constituted by Carbon fibers with rectangular section which are in the three directions of space. These fibers are made up by two or four yarns with 3 000 Carbon filaments each. The voids between fibers are filled up by Carbon, at high pressure and temperature. The section of fibers is not the same in the three directions. The density of material is 2.

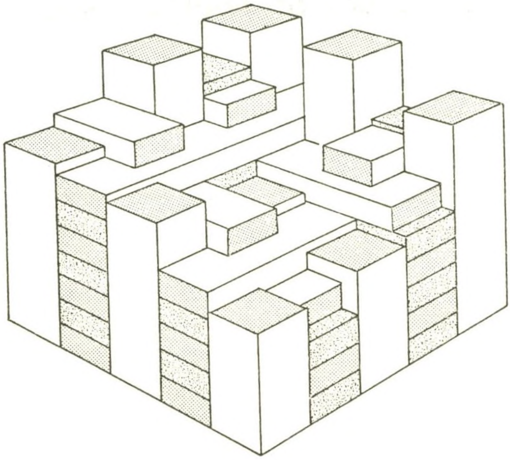

Figure 1 : Geometrical structure of 3DCC

The material has three planes of symetry and, macroscopicaly, it is orthotropic in axes paralleles to fibers ones.

EXPERIMENTAL METHOD

Tests

It is simple traction or compression tests, at room temperature, with monotonic or cyclic loading (unloading to free stress state). The specimens are cut in a plane including fiber directions. We call ϕ the angle between the fiber and loading direction ; the last one is called X. Thus we have, in orthotropic axes, traction or compression-shear stress state.

We have designed specimens and traction or compression loading heads to :
- eliminate the side effects in the gage lenght of the specimen in order to obtain an uniform repartition of stresses,
- have a fixing which does not destroy the material and ensure a good balancing of the specimen,
- prevent the buckling of compression test pieces,
- ensure a homogeneous stress distribution in the heads of specimen by incorporating a soft material (Lead) in the load transmission. Indeed the presence of defects due to the fabrication should involved a load distribution only on few fibers.

The cross area in the gage length fo traction specimens is :
- 3,4 x 6,6mm^2,

and for compression :
- 16 x 16mm^2 and 8 x 8mm^2 ;

these different sections are choosen in order to check an eventual scale effect.

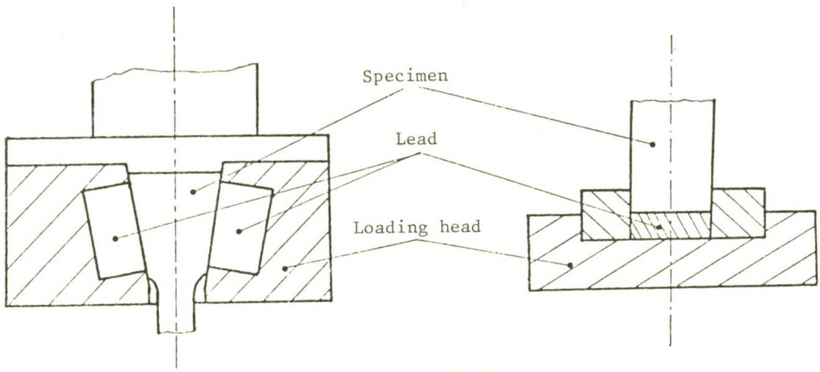

traction specimen and loading head for compression

Figure 2.

METHOD OF MEASURE

By the inhomogeneity of material and the making effects, we cannot have a simple experimental sollicitation of traction or compression in X-direction. They induce important bending effects which are taken into account in the experimental method. We assume we have a traction or compression-bending load (torsion is small). This stress state induces theoritical longitudinal and transversal deformations which are a linear function of the x-y-z coordinates. See (1).

Experimentally, around the specimen and in a same plane, longitudinal and transversal strain gauges are fixed. We determine the best plane through deformations measured at time t. The deformation in the middle point of plane correspond to pure traction or compression tests, without bending. See figures 3, 4.

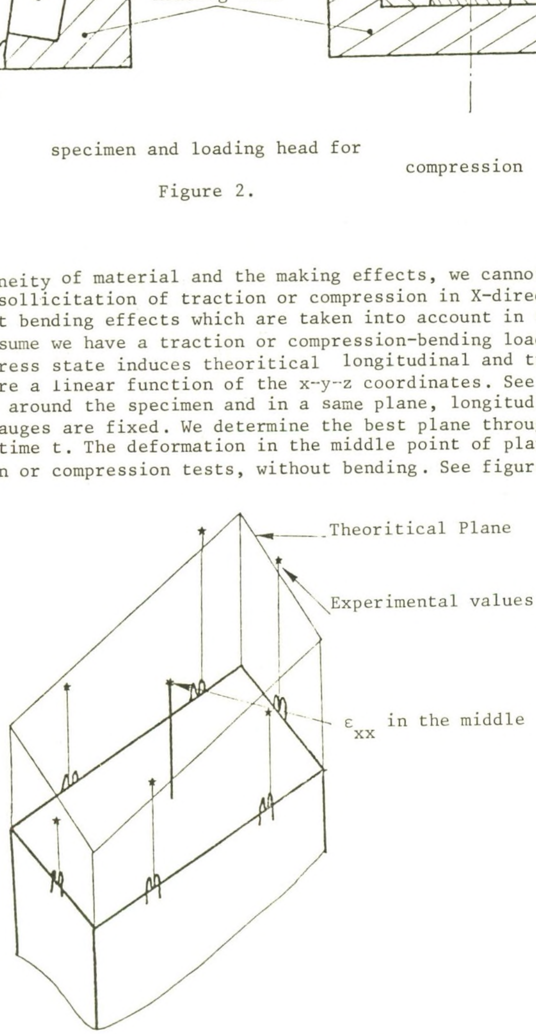

Figure 3 : Plane of deformations through the measures.

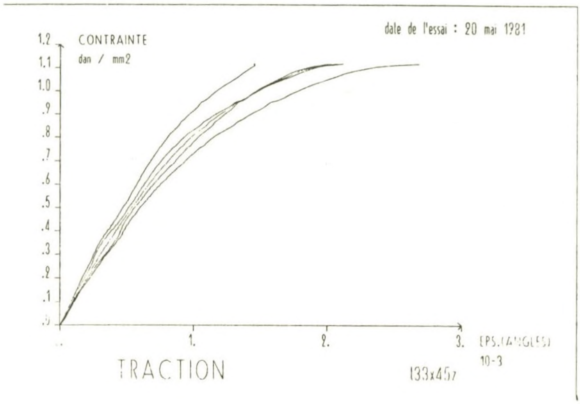

Figure 4 : Experimental curves for the deformations at the middle and four wedges of a cross section (traction test).

This measure of bending makes it possible to qualify a test : for each gauge we can see the divergence between the experimental and numerical deformations, and estimate the importance of bending for a test.

Let σ_{xx} the stress which is the ratio of the applied force to the cross area ; let ε_{xx} the longitudinal deformation and ε_{yy}, ε_{zz} the transversal deformations in the middle of specimen. We can draw the graphs :

$$\varepsilon_{xx} = f(\sigma_{xx}) \qquad \varepsilon_{yy} = f(\sigma_{xx}) \qquad \varepsilon_{zz} = f(\sigma_{xx})$$

The experimental system is constituted by : a testing machine INSTRON with imposed rate of displacement and a data acquisition system HELWET-PACKARD 9825. Results are processed on a UNIVAC 1110.

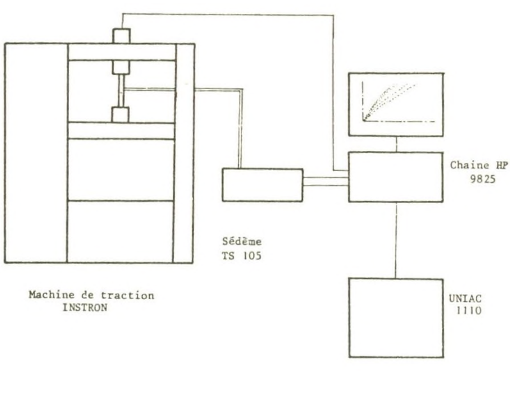

Figure 5 : Experimental system

MODELISATION OF BEHAVIOUR

Let σ and ε the stress and strain tensors. In the axes of specimen, σ is :

$$\begin{bmatrix} \sigma_{xx} & 0 & 0 \\ 0 & 0 & 0 \\ 0 & 0 & 0 \end{bmatrix}$$

The model is built up in the principale material coordinates system. Here, stresses and strains are called σ_{ij} and ε_{ij} with i,j = 1, 2 or 3. This system is obtained from the specimen system by means of a rotation about Z axis through the angle ϕ.

Let $X = (x_1, x_2, x_3)$ the coordinates of a point ; $\vec{u} = \vec{u}(x_1, x_2, x_3)$ is the vector of displacement of this point. ε_{ij} is :

$$\varepsilon_{ij} = \frac{1}{2}\left(\frac{\partial U_i}{\partial x_j} + \frac{\partial U_j}{\partial x_i}\right)$$

Make the assumption that the total deformation ε is the sum of an elastic deformation ε^e and a plastic deformation ε^p :

$$\varepsilon = \varepsilon^e + \varepsilon^p$$

The law of elastic behaviour is orthotropic. Let E_i°, ν_{ij} and G_{ij}° respectively YOUNG's modulus in i-direction, POISSON's ratio and shear modulus in a plane (i,j). We determine these initial elastic values with traction or compression tests at $\phi = 0°$ or $45°$:

$E_i^\circ = 120 \quad 10^3$ MPa

$G_{ij}^\circ = 5{,}5 \quad 10^3$ MPa

$\nu_{ij} \simeq 0.04$

Damage

The notion of damage is due to RABOTNOV-KACHANOV and has been expanded by (2). Damage phenomenon is defined as progressive deterioration of loaded materials, due to the initiation and development of micro-voids and micro-cracks. These defects become visible under microscope if we observed a section of specimen. We can see voids in matrix and fibers, and cracks in fiber-matrix interfaces. Here, damage is revealed by a variation of elastic modulus. Experimentaly we observe this one only on YOUNG's modulus and shear modulus. We have no variation on POISSON's ration, because it is very small. The evolution of damage is found by using cyclic tests. Here we introduce 6 scalar variables such that :

$$\begin{aligned} E_i &= E_i^\circ (1 - D_i) \\ G_{ij} &= G_{ij}^\circ (1 - D_{ij}) \end{aligned} \qquad \text{with } 0 \leqslant D_i \leqslant 1 \qquad (1)$$

E_i° and G_{ij}° are respectively the initials YOUNG's modulus and shear modulus. Then, the law of behaviour is : $\varepsilon = K^{-1}\,\sigma$ or :

$$\begin{aligned} \varepsilon_{ij} &= \frac{\sigma_{ii}}{E_i^\circ (1 - D_i)} - \Gamma_{ij}^\circ \;\sigma_{jj} - \Gamma_{ik}^\circ \;\sigma_{kk} \qquad \text{(i,j,k) permutation of (1,2,3)} \\ \varepsilon_{ij} &= \frac{\sigma_{ij}}{G_{ij}^\circ (1 - D_{ij})} \qquad (i \neq j) \end{aligned} \qquad (2)$$

E_i°, G_{ij}°, et Γ_{ij}° are constants

D_i and D_{ij} will be denoted $\mathbb{D}$: $\mathbb{D} = (D_1, D_2, D_3, D_{12}, D_{23}, D_{13})$

Thermodynamical approach

Let Ψ the free energy of material, we assume that Ψ depends on elastic deformation ε^e , hardening parameter P and damage variables $\mathbb{D}$.
ρ is the voluminal mass of material.

$$\rho\,\Psi\,(\varepsilon^e, \mathbb{D}, P) = W_e\,(\varepsilon^e, \mathbb{D}) + \phi(P) \tag{3}$$

and W_e is elastic energy :

$$W_e\,(\varepsilon^e, \mathbb{D}) = \frac{1}{2}\,\varepsilon^e : K\varepsilon^e \tag{3'}$$

For this relation we made the assumption of the separation between damage and hardening parameters. To verify the second law of thermodynamics, we must satisfy the CLAUSIUS-DUHEM inequality :

$$-\rho\,\dot{\Psi} + \sigma : \dot{\varepsilon} > 0 \tag{4}$$

where $\dot{\nu}$ is the derivative of ν with respect to time t. It follow from rel.(2) and (3) that :

$$\sigma : \dot{\varepsilon} - \mathbf{Y} : \mathbb{D} - R\dot{P} > 0 \tag{5}$$

with

$$\mathbf{Y} = + \frac{\partial We}{\partial \mathbb{D}} \qquad R = \frac{\partial\,\phi}{\partial\,P}$$

a sufficient condition to satisfy rel. (5) is :

$$\begin{array}{lll} -\,\mathbf{Y} : \dot{\mathbb{D}} > 0 & & \text{damage dissipation} \\ \sigma : \dot{\varepsilon}^p - R\dot{P} > 0 & & \text{plastic dissipation} \end{array} \tag{6}$$

we verify, by (3') and (5), that $(-\mathbf{Y})$ is positive. As the evolution of damage is positive because this one increases with time, we have the first inequality (6). The model must satisfy the second one.

Traction and compression behaviour $(\sigma_{ii} \neq 0,\ \sigma_{ij} = 0 \text{ if } i \neq j)$

An experimental traction curve at $\phi = 0°$ is given figure 6. We see that we have a brittle linear elastic behaviour. In compression this one is very different : when we examine cyclic tests, figure 7, we note that the residual deformation equal to zero ($\varepsilon_{ii} = 0$) at free stress. Therefore the plastic deformation ε^p_{ii} is zero. It is YOUNG's modulus variation which gives the non-linearity of behaviour. In compression the model is non-linear elastic with damage.

$$\varepsilon_{ii} = \varepsilon^e_{ii} = \frac{\sigma_{ii}}{E^\circ_i\,(1 - D_i)} \tag{7}$$

$$\begin{array}{lll} \text{where } D_i = 0 & \text{if } \sigma_{ii} > 0 & \\ & \text{if } \sigma_{ii} < 0 \text{ and } \sigma^*_{ii} \leqslant |\sigma^e_{ii}| & \\ \quad = -\dfrac{(\sigma^*_{ii} - \sigma^e_{ii})}{a} & \text{if } \sigma_{ii} < 0 \text{ and } \sigma^*_{ii} > |\varepsilon^e_{ii}| & \end{array} \tag{8}$$

$\sigma^*_{ii} = \sup\limits_{\tau<t} \langle \sigma_{ii} \rangle_-$ where $\langle a \rangle_-$ is the negative part of a

σ^e_{ii} is elastic limite in compression

we have : $a = 300$ MPa $\qquad \sigma^e_{ii} = -10$ MPa

In rel.(7) we have disregarded the constants Γ°_{ij} because ν_{ij} is very small. The rupture criterions are : in traction $\varepsilon_{ii} \leqslant \varepsilon^*_{ii}$ where ε^*_{ii} is the rupture strain, in compression $D_i \leqslant D^{c*}_i$ where D^{c*}_i is the critial damage in i-direction.

$$\varepsilon^*_{ii} = 2.10^{-3} \qquad D^{c*}_i = 0.23$$

The law of D_i in compression, is given by figure 8.

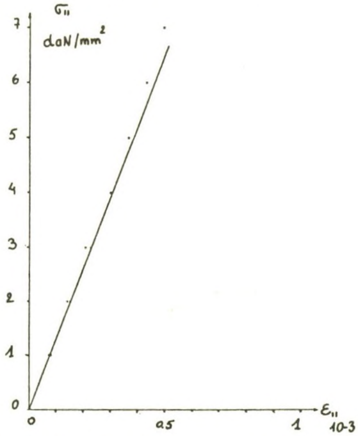

Figure 6 : Traction curve for $\phi = 0°$

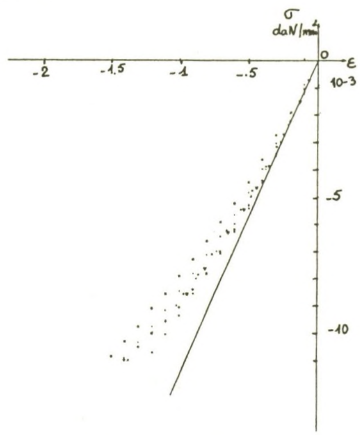

Figure 7 : Compression curve for $\phi = 0°$

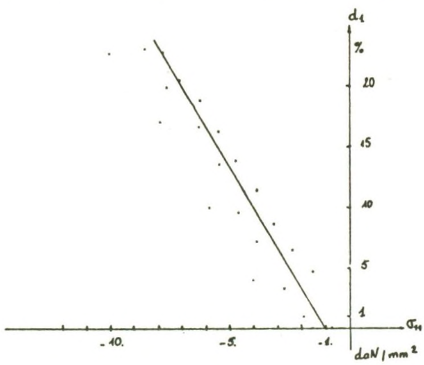

Figure 8 : Evolution of D_i function of σ_{ii}

Remarks : The modelisation of traction or compression behaviour reveals two important hypothesis which are the foundations of model :

- separation between traction and compression behaviour.
- use of the most simple extension of unidimensional tests to a tridimensional behaviour. We apply these ones to the shear behaviour.

<u>Shear behaviour</u> $(\sigma_{ij} \neq 0)$

Put $$\varepsilon_{ij} = \varepsilon^{e}_{ij} + \varepsilon^{p}_{ij} = h_{ij}(\sigma_{ij}) \qquad (9)$$

The function h_{ij} is determined from experimental curves $\varepsilon_{xx} = f(\sigma_{xx})$ and $\varepsilon_{yy} = f(\sigma_{xx})$ by using the following relations, here in a plane (1,2) :

$$\varepsilon_{xx} = \left(\frac{\cos^4\phi}{E_1} + \frac{\sin^4\phi}{E_2}\right) \sigma_{xx} - 2h_{12}(-\sigma_{xx} \sin\phi \cos\phi) \sin\phi \cos\phi$$

$$\varepsilon_{yy} = \sin^2\phi \cos^2\phi \left(\frac{1}{E_1} + \frac{1}{E_2}\right) \sigma_{xx} + 2h_{12}(-\sigma_{xx} \sin\phi \cos\phi) \sin\phi \cos\phi$$

h_{ij} is determined from tests at $\phi = 45°$, for σ_{xx} positive and negative. See fig. 9.

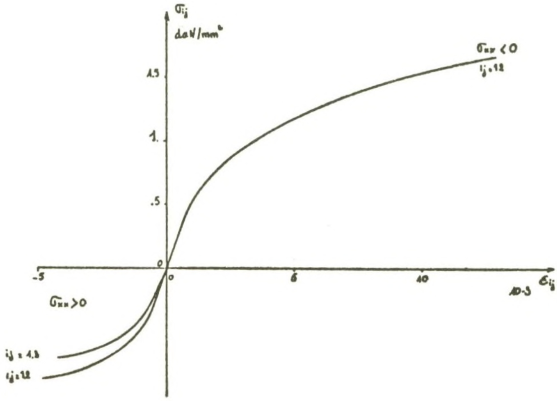

Figure 9 : Shear behaviour

On cyclic curves, we remark the existence of damage and plastic phenomenons : damage by the variation of shear modulus due to the micro-cracks in fiber-matrix interface, plasticity by residual deformations increasing with σ_{ij}. The evolution curves of D_{ij}, see rel. (2), are drawn fig.10 for σ_{xx} positive and negative.

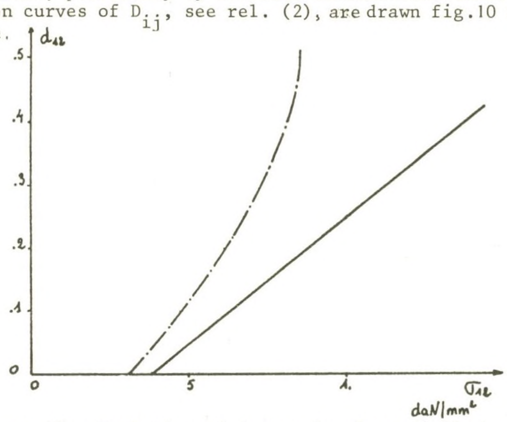

Figure 10 : Evolution of damage in plane (1,2) for shear.
—·—·— $\sigma_{xx} > 0$; ———— $\sigma_{xx} < 0$

We observe that the damage in traction is larger than in compression. We can explain this difference by the effect of hydrostatic pressure on micro-voids and micro-cracks : indeed, by this pressure, the defects grow in tension whereas in compression the voids tend to close and the cracks growth is lesser.
The model fo damage is :

$$\varepsilon^e_{ij} = \frac{\sigma_{ij}}{G^\circ_{ij}\ (1 - D_{ij})} \qquad (11)$$

$$\text{with } D_{ij} = 0 \qquad \text{if } \sigma^*_{ij} < |\sigma^e_{ij}|$$

$$= L^1_{ij}\ (\sigma^*_{ij}) + L^2_{ij}\ (P^*) \quad \text{if } \sigma^*_{ij} > |\sigma^e_{ij}| \qquad (12)$$

where $L^2_{ij}(P^*) = 0$ if $P < 0$

> 0 if $P > 0$ (13)

P is the hydrostatic pressure, here $P = \frac{\sigma_{xx}}{3}$

$$P^* = \sup_{\tau<t} \langle P \rangle_+ \qquad \sigma^*_{ij} = \sup_{\tau<t} (|\sigma_{ij}|)$$

the identification gives :

$$L^2_{ij}(\sigma^*_{ij}) = \frac{\sigma^*_{ij} - \sigma^e_{ij}}{b} \quad ; \quad L^1_{ij}(P^*) = \left(\frac{P^* - Po}{K}\right)^N \tag{14}$$

with b = 25 MPa   Po = 2 MPa   K = 7,5 MPa   N = 1.7 σ^e_{12} = 3.8 MPa for the plane (1,2). We cannot give the results in the three planes because some tests have not be done.

Now , if we draw the experimental curves of plastic deformations ε^p_{ij} function of σ_{ij} we have not the same curve for σ_{xx} positive or negative. But we obtain a single curve if we plot plastic deformation against :

$$\frac{\sigma_{ij}}{1 - D_{ij}} = \tilde{\sigma}_{ij}.$$

Only the rupture stresses are not the same.

From this result, a plastic model with isotropic hardening is built up. See (3). This model verify the second inequalit y (6). We introduce a scalar function g :

$$g = \tilde{\sigma}_{II} - L(P')$$

where $\tilde{\sigma}_{II} = \sqrt{2}\left(\tilde{\sigma}^2_{12} + \alpha^2\,\tilde{\sigma}^2_{23} + \beta^2\,\tilde{\sigma}^2_{13}\right)^{1/2}$ (15)

such that $\dot{\varepsilon}^p_{ij} = \lambda \frac{\partial g}{\partial \tilde{\sigma}_{ij}} \qquad P' = -\lambda \frac{\partial g}{\partial L}$ (16)

L(P') is characteristic of the material.

α and β are parameters which distinguish the behaviour in the planes (1,2), (2,3), and (3,1).

$\lambda = 0$ if $g < 0$ or $g = 0$, $\dot{g} < 0$ elastic behaviour

> 0 if $g = \dot{g} = 0$ plastic behaviour (17)

λ is determined by the condition $\dot{g} = 0$

It follow from (15), (16) and (17) that :

$$P' = \frac{1}{\sqrt{2}} \int_0^t \left\{ (1 - d_{12})^2\, \dot{\varepsilon}^{p2}_{12} + \frac{(1 - d_{23})^2}{\alpha^2}\, \dot{\varepsilon}^{p2}_{23} + \frac{(1 - d_{13})^2}{\beta^2}\, \dot{\varepsilon}^{p2}_{13} \right\}^{1/2} dt \tag{18}$$

We identify the function L(P') with tests at $\emptyset$ = 45° in plane (1,2). See fig.11.

$$\tilde{\sigma}_{12} = \frac{1}{\sqrt{2}} L \left(\frac{1}{\sqrt{2}} \int_0^t (1 - d_{12})\, \dot{\varepsilon}^p_{12}\, dt \right) \tag{19}$$

The values of α and β are given by the curves in plane (2,3) and (3,1). For the Carbon-Carbon composite that we have tested :

$$\alpha = \beta = 1.2$$

The model, identified by the tests at $\emptyset$ = 0° and $\emptyset$ = 45°, has been verified on tests at $\emptyset$ = 30°. The comparison between experimental and theoritical results is given figure 12.

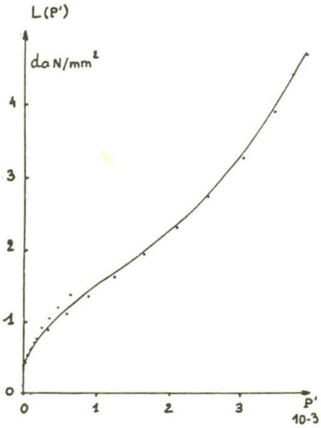

Figure 11 : Identification of L(P)

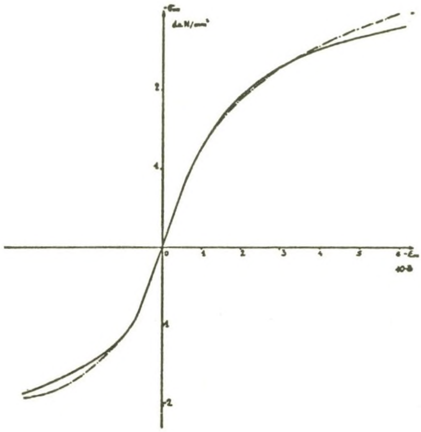

Figure 12 : Theoritical and experimental results for Ø = 30°

CONCLUSION

From simple sollicitations, a model has been built up. It distinguishes traction, compression and shear behaviour. Important damage phenomenons have been noticed, even if the deformations are small. This can be explained by a great density of micro-voids and micro-cracks in initial material. A more precise analysis is still to be done on tridimensional tests (for example traction or compression torsion).

REFERENCES

1 Ladevèze, P., "Sur la théorie des poutres droites élastiques homogènes et anisotrope" to appear.

2 Lemaitre, J. and Chaboche J.L., "Aspect phénoménologique de la rupture par endommagement", J. de Mécanique Appliquée, Vol. 3, 1978, pp. 317-360

3 Halphen, B. and Nguyen Quoc Son, "Sur les matériaux standards généralisés", J. de Mécanique, Vol. 14, N° 1, 1975, pp 39-63

4 Ladevèze, P. and Poss, M. and Proslier, L., "Comportement mécanique non linéaire des matériaux 3D Carbone-Carbone", rapport de contrat S.N.I.A.S. n° 8944-4400, 1981

5 Ladevèze, P. and Poss, M. and Proslier, L., " Sur l'endommagement et la rupture des matériaux composites 3D", rapport de contrat S.N.I.A.S. n° 9554-4400, 1982

6 Poss, M., Thèse de 3ème cycle, 1982

7 Perry and Adams, "Mechanical test of a three dimensionally reinforced Carbon-Carbon Composite Matérials, Carbon G.B., N° 1, 1976

8 Crawford and Lawrence, "Multidirectionaly reinforced Carbon-Carbon Composites", Lachman, Mab.Internaltional.